

Retraction

Retracted: Fast and Accurate Position Determination of Multimodal Couplings of Steel Rolling Machinery and Equipment Combined with Multimedia Optimized Particle Filters

Advances in Multimedia

Received 15 August 2023; Accepted 15 August 2023; Published 16 August 2023

Copyright © 2023 Advances in Multimedia. This is an open access article distributed under the Creative Commons Attribution License, which permits unrestricted use, distribution, and reproduction in any medium, provided the original work is properly cited.

This article has been retracted by Hindawi following an investigation undertaken by the publisher [1]. This investigation has uncovered evidence of one or more of the following indicators of systematic manipulation of the publication process:

- (1) Discrepancies in scope
- (2) Discrepancies in the description of the research reported
- (3) Discrepancies between the availability of data and the research described
- (4) Inappropriate citations
- (5) Incoherent, meaningless and/or irrelevant content included in the article
- (6) Peer-review manipulation

The presence of these indicators undermines our confidence in the integrity of the article's content and we cannot, therefore, vouch for its reliability. Please note that this notice is intended solely to alert readers that the content of this article is unreliable. We have not investigated whether authors were aware of or involved in the systematic manipulation of the publication process.

Wiley and Hindawi regrets that the usual quality checks did not identify these issues before publication and have since put additional measures in place to safeguard research integrity.

We wish to credit our own Research Integrity and Research Publishing teams and anonymous and named external researchers and research integrity experts for contributing to this investigation.

The corresponding author, as the representative of all authors, has been given the opportunity to register their

agreement or disagreement to this retraction. We have kept a record of any response received.

References

- [1] J. Tan, "Fast and Accurate Position Determination of Multimodal Couplings of Steel Rolling Machinery and Equipment Combined with Multimedia Optimized Particle Filters," *Advances in Multimedia*, vol. 2021, Article ID 3693503, 7 pages, 2021.

Research Article

Fast and Accurate Position Determination of Multimodal Couplings of Steel Rolling Machinery and Equipment Combined with Multimedia Optimized Particle Filters

Jian Tan 

Wuhan Huaxia University of Technology, Wuhan 430223, China

Correspondence should be addressed to Jian Tan; chen159346wu843@163.com

Received 15 August 2021; Accepted 9 November 2021; Published 11 December 2021

Academic Editor: Zhendong Mu

Copyright © 2021 Jian Tan. This is an open access article distributed under the Creative Commons Attribution License, which permits unrestricted use, distribution, and reproduction in any medium, provided the original work is properly cited.

During the overhaul and maintenance of the transmission system of the modern rolling mill, a very common problem is the positioning of the motor and the reducer or speed increaser. The operation of the equipment and the service life of the equipment will be significantly affected by the accuracy of the multimodal coupling position determination. Therefore, precise positioning and rapid positioning must be achieved. This article intends to analyze how this type of equipment achieves rapid and accurate positioning and what factors will affect the location determination process.

1. Introduction

With the continuous development of my country's market economy, the steel industry has also been rapidly improved, the automation level of the entire industry has been continuously improved, and the high-speed and continuous characteristics of the industry are very prominent, and the importance of equipment operation safety has become increasingly prominent [1–3]. Based on the current background, it is urgent to strengthen the application of the rapid and accurate position determination technology of modern multimodal couplings to achieve precise positioning. Since the founding of the People's Republic of China, the country's steel industry has developed vigorously, but there have also been many problems in the process. For example, equipment damage caused by vibration will not only affect the entire production plan but also the product quality will not be guaranteed. Mechanical vibration can help to understand the overall situation of mechanical equipment. At present, when quickly determining the position of the equipment, the most commonly used method is to detect the vibration signal. The proposal and application of this technology have also greatly changed the way equipment is maintained. Up to now, only

some simple machines have applied this technology, but specific to large equipment, such as rolling mills, the fast and accurate position determination technology of multimodal couplings is still immature [4, 5].

Check the installation plane of the base and the ground of the motor foot mainly to judge whether there are high points and burrs and to judge its smoothness and flatness. If these problems are found, corresponding measures must be taken to deal with them in time; otherwise, it will have a greater impact on the accuracy of the position determination, or the final position determination data will be distorted. Although the final accuracy data deviation still meets the relevant requirements, there will be obvious vibrations during the operation of the equipment. The measurement method is as follows: freely place the motor on the base, check the contact surface between the base and the base, and check whether there is any around the foot to determine whether it is flat contact or not, if the foot is lifted, suspended in the air, etc. If there is dangling, use a feeler gauge to measure the dangling value. For the dangling margin, use the foot pad to compensate. Generally, the thickness of the pad is higher than the measured value of the feeler gauge, generally 0.1 ~ 0.15 mm, the purpose is to ensure that the foot can be cushioned firmly. In

particular, some electrical equipment has undergone many repairs and the bottom plate has been deformed, or the foundation has settled because of the age. This must be ensured to avoid adding additional burdens to the feet and affecting the operation of the electrical equipment, which in turn affects the life of the motor.

2. Fast and Accurate Position Determination System Structure

Figure 1 shows the specific process of the rapid and accurate location determination system, which is mainly divided into three stages: monitoring, rapid and accurate location determination, and prevention [6, 7]. No specific introduction here, the following will focus on the principles and algorithms applied in the fast and accurate position determination system. The basic principle of the spectrum analysis method is the fast Fourier transform, which is also the origin of its other name, the multimedia optimized particle filter analysis method. The fast Fourier transform can effectively reduce the amount of N -point DFT calculations, that is, from N^2 times to $(N/2)\log_2^N$ times. The principle is the periodicity and symmetry of the rotation factor w . The specific definition of DFT is as follows:

$$X(k) = \sum_{n=0}^{N-1} x(n)W_N^{nk}, \quad k = 0, 1, \dots, N-1. \quad (1)$$

Among them, $x(n)$ belongs to the complex sequence and the length is N . It can be found from the above formula that the N -point DFT needs to perform multiple multiplications and additions. If N is relatively large, it means that a more complicated budget is required. The core idea of the multimedia optimized particle filter is as follows: decompose the original N -point sequence to obtain several short sequences, and recombine the DFT of these short sequences to obtain the DFT of the original sequence. This article focuses on the two extraction algorithms based on time.

Set $N = 2^M$, M to be a positive integer. Group $X(n)$ according to parity, and get two groups: let $n = 2r$ and $n = 2r + 1$, $r = 0, 1, \dots, N/2 - 1$, thus we can get

$$X(k) = \sum_{r=0}^{N/2-1} x(2r)W_{N/2}^{rk} + W_N^k \sum_{r=0}^{N/2-1} x(2r+1)W_{N/2}^{rk}, \quad (2)$$

where $W_{N/2} = e^{-j(2\pi/(N/2))} = e^{-j4\pi/N}$ makes

$$A(k) = \sum_{r=0}^{N/2-1} x(2r)W_{N/2}^{rk}, \quad k = 0, 1, \dots, \frac{N}{2} - 1, \quad (3)$$

$$B(k) = \sum_{r=0}^{N/2-1} x(2r+1)W_{N/2}^{rk}, \quad k = 0, 1, \dots, \frac{N}{2} - 1,$$

then $X(k) = A(k) + W_N^k B(k)$, $k = 0, 1, \dots, N/2 - 1$.

Since $A(k)$ and $B(k)$ are both $N/2$ -point DFT, and $X(k)$ is N -point DFT, there should also be

$$X\left(k + \frac{N}{2}\right) = A(k) - W_N^k B(k), \quad k = 0, 1, \dots, \frac{N}{2} - 1. \quad (4)$$

In this way, $A(k)$ and $B(k)$ can be used to completely express $X(k)$. Compared with DFT, this method is easier to implement, has a smaller amount of calculation, and greatly enhances the convenience of engineering calculations.

3. Fast and Accurate Position Determination of Multimodal Couplings of Steel Rolling Machinery and Equipment

When performing multimedia optimization particle filter spectrum analysis, $\Delta f = f/n$ represents the frequency resolution, where n represents the number of sampling points, and f represents the sampling frequency and meets $f \geq 2f_{\#}$ ($f_{\#}$ represents the highest sampling frequency) [8–10]. When applying this technical method to engineering, first install an acceleration sensor at the detection position. After the sensor is processed by an amplifier and filter, it will be transferred to the computer, which can realize the spectrum analysis in the MATLAB environment and present the results. To determine the cause of the failure of the rolling mill [11, 12], Figure 2 is a specific flow chart.

- (1) Installation and fixing of dial indicator and bracket: before installation, you need to check the dial indicator first to ensure that it is flexible and accurate and that the side head is complete and smooth. The specific operation is as follows: push the dial indicator's measuring rod by hand, and the index changes steadily. There is no jamming problem. In addition, it is necessary to ensure that the centripetal scale and the bracket are stable. Check this to ensure that the rigidity is sufficient to ensure that the rotation of the multimodal coupling will not cause an error in the indication due to the excessively large bracket. Figure 3 shows the specific installation methods of the two dial indicators.
- (2) Crank readings and record the values: combined with Figure 4, record $d_1, r_1; d_2, r_2; d_3, r_3; d_4, r_4$. During data recording, this article recommends that the driving shaft and the driven shaft rotate at the same time, although some multimodal couplings are equipped with special high-precision machining surfaces that can be used to determine the position. In this case, you can only rotate the motor axis to read the value. However, in reality, especially during maintenance, various collisions will inevitably occur when the equipment is installed, and problems such as deformation will also occur during the use of the equipment, and errors may also occur during processing, which will become positions. Determine the error source of the data. Therefore, it is not recommended to fix one end of rotation when recording the data in this article.

The read value should meet: $d_1 + d_3 = d_2 + d_4$; $r_1 + r_3 = r_2 + r_4$; if the difference between $d_1 + d_3$ and $d_2 + d_4$ is too large (greater than 0.02 mm), you need to check the dial indicator and the situation of the stent. If the values of $r_1 + r_3$ and $r_2 + r_4$ differ too much, in addition to checking the dial indicator and the bracket, it is also necessary to consider whether the axis I and axis II are moving. If there is a jump, you need to consider the quality of equipment spare parts or use the three-meter method to determine the location of the equipment.

- (3) Measure and determine the size of the two foundation pads: there are many cases of two-axis deviation. Specifically, there are two main types: opening deviation and outer edge deviation, which are the axial deviation and radial deviation of the two multimodal couplings. When determining the position, the basic principle is as follows: first, adjust the upper and lower numerical deviation, and then adjust the left and right deviation. Taking into account that when adjusting the gasket, the direction of the left and right deviations is uncertain. At this time, compared with the reducer (axis I), the motor (axis II) is lower, and the multimodal coupling is opened on the device.

Step 1. Adjust the axis II and move it upward so that it is at the same height as the axis I, that is, 0, and the same height as 0. At this time, the two anchors need to increase the size of the film:

$$e_1 = e_2 = e. \quad (5)$$

Among them, $e = (1/2)(d_1 - d_3)$.

Step 2. Use the adjusted 0 as the base point to rotate the axis II. After the rotation, the two axes are required to be collinear. Combined with Figure 2, based on the characteristics of similar triangles, it can be calculated:

$$\begin{aligned} \frac{S}{D} &= \frac{X_1}{L_1} = \frac{X_2}{L_1 + L_2}, \\ X_1 &= \frac{S}{D} \cdot L_1, \\ X_2 &= \frac{S}{D} (L_1 + L_2). \end{aligned} \quad (6)$$

Among them, $S = r_3 - r_1$.

D: 2 times the distance between the measuring point of the dial indicator and the center of rotation of the shaft.

Step 3. Use Δ_1 and Δ_2 to indicate the size of the spacers of foot 1 and foot 2 to be increased, and the calculation formula is as follows:

$$\begin{aligned} \Delta_1 = e + X_1 &= \frac{1}{2} (d_1 - d_3) + \frac{r_3 - r_1}{D} \cdot L_1, \\ \Delta_2 = e + X_2 &= \frac{1}{2} (d_1 - d_3) + \frac{r_3 - r_1}{D} \cdot (L_1 + L_2). \end{aligned} \quad (7)$$

If the development of the active shaft appears to jump or the passive shaft has such a situation, or the position determination accuracy requirements are particularly high, then the position determination can be carried out by the three-meter method at this time. After the dial indicator is installed, Figure 5 can be obtained. There is no difference between the calculation of the outer marginal difference when using the three-meter method and the double-meter method for the position value determined by the three-meter method. The opening deviation can be calculated according to the following formula:

$$S = (r_3 + r'_3) - (r_1 + r'_1). \quad (8)$$

If the result calculated by the above formula is greater than zero, it is expressed as the upper opening; otherwise, it is the lower opening; the final goal to be achieved after adjustment is $r_1 + r'_1$ and $r_3 + r'_3$; $r_2 + r'_2$ and $r_4 + r'_4$. The value is the same or meets the required accuracy range.

The calculation and pad adjustment method is the same as the double table method.

4. Examples and Results Analysis

For the precise positioning of multimodal couplings, compared with other methods, the multimedia optimized particle filter is effective, and its effectiveness is verified here [13, 14]. Specifically, this article uses two simulation cases of precise positioning of multimodal couplings to verify the multimedia optimization particle filter. The comparison is mainly carried out from the two levels of no error level and tracking performance: first of all, tracking the maneuvering target moving in a uniform linear motion on the simulated xy plane; secondly, simulation experiments were carried out on EKF, UKF, and PF. The state transition equation is

$$\begin{bmatrix} x_{k+1} \\ x'_{k+1} \\ y_{k+1} \\ y'_{k+1} \end{bmatrix} = \begin{bmatrix} 1 & \frac{\sin \omega T}{\omega} & 0 & \frac{1 - \cos \omega T}{\omega} \\ 0 & \cos \omega & 0 & -\sin \omega T \\ 0 & \frac{1 - \cos \omega T}{\omega} & 1 & \frac{\sin \omega T}{\omega} \\ 0 & \sin \omega T & 0 & \cos \omega T \end{bmatrix}_k \begin{bmatrix} x_k \\ x'_k \\ y_k \\ y'_k \end{bmatrix} + \begin{bmatrix} \frac{T^2}{2} & 0 \\ T & 0 \\ 0 & \frac{T^2}{2} \\ 0 & T \end{bmatrix}_k \omega_k. \quad (9)$$

The state transition equation reflects that a maneuvering target on the xy plane is in a nonlinear motion state, the target position is (x, y) , the turning speed model is $\omega_{k+1} = \omega_k + w_{\omega,k}$, T is the sampling interval, and $w_k, w_{\omega,k}$ is the system noise. The measurement equation is shown below:

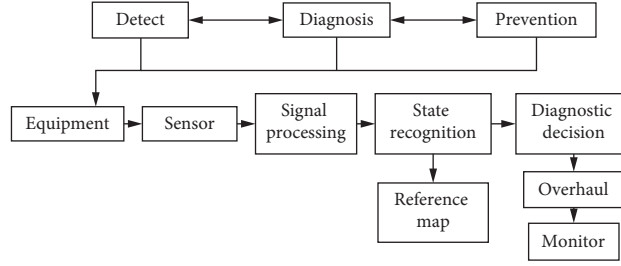


FIGURE 1: Flow chart of fast and accurate location determination.

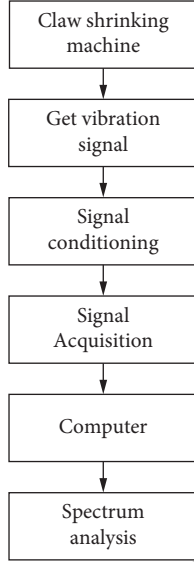


FIGURE 2: Flow chart.

$$\begin{cases} r_k = \sqrt{x_k^2 + y_k^2} + v_{k,r}, \\ \theta_k = \arctan(y_k/x_k) + v_{k,\theta}, \\ \dot{r}' = \frac{(x_k x'_k + y_k y'_k)}{\sqrt{x_k^2 + y_k^2} + v_{k,r}}. \end{cases} \quad (10)$$

In the above formula, r and θ respectively represent the slant distance and azimuth angle of the target, and \dot{r} represents the rate of change of the distance. The measurement noise is expressed as $v_k = (v_{k,r}, v_{k,\theta}, v_{k,r})$. At the same time, because the main purpose of this research is to explore the filtering and tracking of the state, the research assumes that the system satisfies the characteristics of the first-order Markov process at this time, and the observations are independent of the known state quantities. The probability density can be expressed as

$$\begin{aligned} p(x_k | x_{0:k-1}) &= p(x_k | x_{k-1}), \\ p(y_k | x_{0:k}) &= p(y_k | x_k). \end{aligned} \quad (11)$$

The settings of some parameters here are as follows: k is 10, α is 1, and β is 2. The simulation environment is as follows:

first, track a uniform straight line target, the entire simulation time is 200 s, the sampling frequency is 1 Hz, the number of particles is 1000, and the initial position is at the origin, that is, the single observing station moves in a uniform straight line from the origin, the initial heading is 30° . Standing on the origin, moving in a straight line counterclockwise, the initial speed is 15 m per second, the distance is 10,000 m, the azimuth is 60° , and the heading angle is 150° . The observation noise and system noise in the simulation process are Gaussian white noise, the mean square error of the observation azimuth noise is 1° , and the mean square error of the system noise is 0.01 m. In the initial stage, the estimated initial value x_0 of the multimedia optimized particle filter can be obtained by the pseudolinear method, and the prior probability $p(x_0)$ can be obtained. This paper has carried out 100 simulation experiments to obtain the tracking curves of the four algorithms shown in Figures 6 and 7.

Combined with the simulation results, it can be found that EKF and UKF have large deviations before maneuvering at the observatory, and the overall characteristics are divergent; and after maneuvering at the observatory, the two algorithms show slow convergence characteristics, but the deviation still exists, resulting in unsatisfactory tracking results. Combining PF and multimedia to optimize the particle filter curve, it can be found that the tracking effect of the particle-based filter is better compared with the two algorithms of EKF and UKF. Before the observation station is maneuvered, although it does not show the characteristics of convergence, it has better convergence than the previous two algorithms. However, when the observation station is maneuvering, the influence of the sudden change of the sensor observation value on the multimedia optimization particle filter is more obvious. The PF filter error level is significantly increased after the observation station is maneuvered. However, the multimedia optimized particle filter uses UKF and EKF to generate the recommended distribution, which has better adaptability to the sudden change of observations, and RMES can quickly reduce.

Figure 8 shows the simulation analysis results of the four algorithms. The initial simulation conditions are as follows: the measuring point starts from the origin of the coordinates, the initial position and speed are $x_0 = [0, 0, 0, 100]^T$, and the turning angular velocity of the maneuvering target is 3° per second. The system noise covariance matrix and the observation noise covariance matrix are $\text{diag}([5, 0.1, 5, 0.1])$

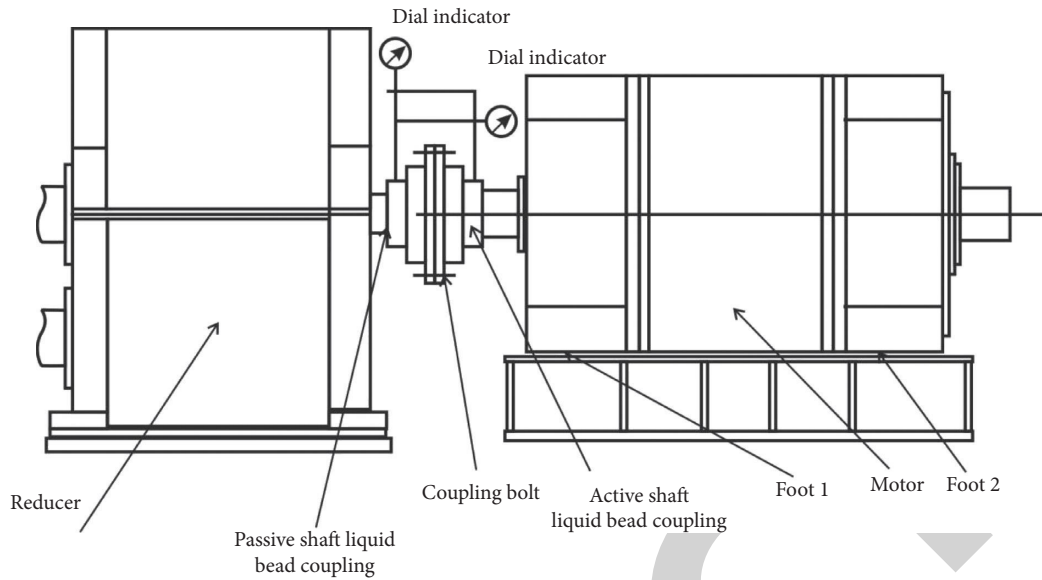


FIGURE 3: Schematic diagram of dial indicator installation and fixing method.

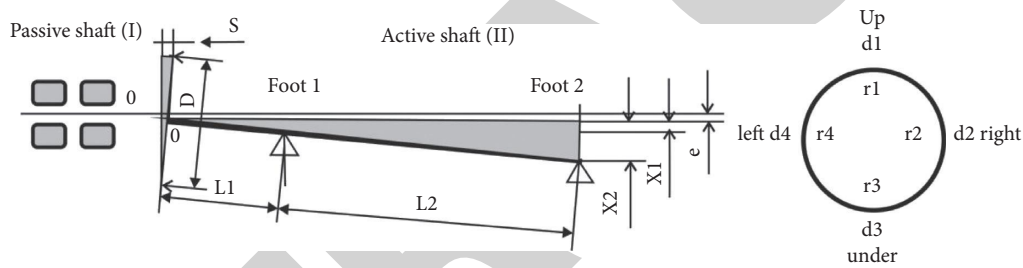


FIGURE 4: Double table method position determination calculation and value recording diagram.

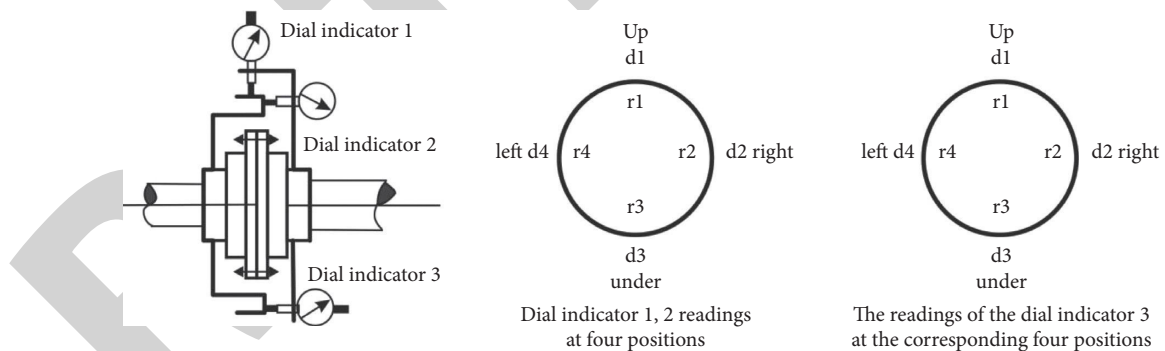


FIGURE 5: Schematic diagram of setting up the position determination dial indicator with three-meter method and the data recording diagram of position determination.

and $\text{diag}([200,0.1])$ in sequence, the sampling interval is 1 s, and the sampling time is 60 s.

Because the trajectories are very close, it is difficult to accurately analyze the changes. Based on this, this study mainly measured the deviation level between the actual position of the track and the estimated position when sampling. In combination with Figure 8, it can be found that the EKF algorithm has a relatively large error level due to the linearization loss; and specifically for PF, because in the

updated observations, the proposed distribution does not contain new observation information; therefore, ideal tracking performance has not been obtained. Compared with the PF, EKF, and UKF algorithms, the performance of the multimedia optimization particle filter algorithm is better, because the algorithm makes full use of all the measurement information, so it has the performance of other filtering algorithms. Both the EKF and UKF algorithms will generate recommended distributions. For

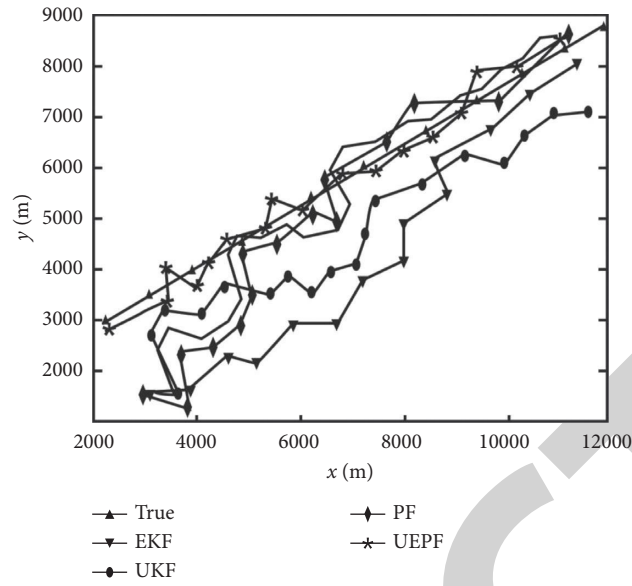


FIGURE 6: Tracking of uniform linear motion trajectory.

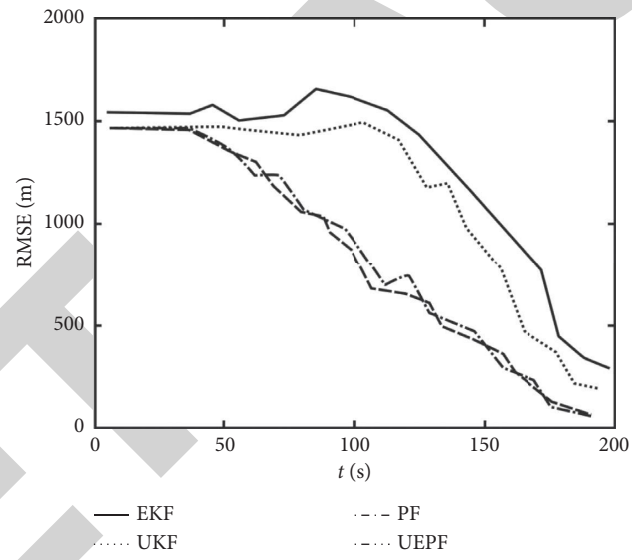


FIGURE 7: RM SE comparison.

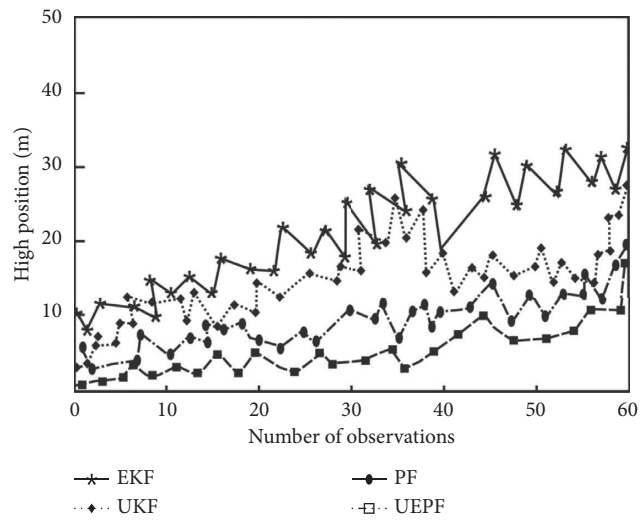


FIGURE 8: The position error of the target during the turn.

multimedia optimized particle filters, in order to ensure better azimuth performance, multiple particles must be processed, and Jacobian matrix calculations must be performed multiple times. This increases the filtering time. However, the average time at each sampling point is 0.2 s, which is 7% to 20% of the observation time, which also meets the real-time requirements in practical applications; secondly, with regard to increasingly complex calculation problems, computer information technology continues to develop, enough to solve this problem.

5. Conclusions

Currently, there are a variety of methods available for determining the position of the motor and the reducer, but most of them require more tedious calculations. For those large-scale steel rolling machinery and equipment, these algorithms are not suitable for follow-up or maintenance. The algorithm proposed in this paper helps to determine the position more efficiently and also clarifies the key points of each link, the accuracy of the position determination is effectively guaranteed, and the practical guiding significance is prominent.

Data Availability

The data used to support the findings of this study are available from the corresponding author upon request.

Conflicts of Interest

The authors declare no conflicts of interest.

Acknowledgments

This research study was sponsored by the following projects: (1) The project of excellent young and middle-aged science and technology innovation team of colleges and universities in Hubei province: Advanced Design and Manufacturing Technology, the project number: T201837, Project Leader is Qi Hongfang. (2) "Jingchu Outstanding Talents" Collaborative education Program for ordinary undergraduate universities in Hubei Province: Mechanical Design, Manufacturing and Automation Major, Wuhan Huaxia University of Technology, the project number: "Letter of higher education in Hubei Province" [2017] No. 29, Project Leader is Qi Hongfang. The authors would like to thank these projects for supporting this article.

References

- [1] H. Li, J. Gu, A. Hanif, A. Dhanasekar, and K. Carlson, "Quantitative decision making for a groundwater monitoring and subsurface contamination early warning network," *The Science of the Total Environment*, vol. 683, no. 15, pp. 498–507, 2019.
- [2] S. Benjamin and J. Manfred, "Combining network and array waveform coherence for automatic location: examples from induced seismicity monitoring," *Geophysical Journal International*, vol. 3, pp. 1373–1388, 2017.
- [3] X. Ni, "Management and maintenance of computer room in university," *China Computer & Communication*, vol. 51, no. 17, pp. 489–494, 2017.
- [4] E. Intrieri, G. Gigli, M. Nocentini et al., "Sinkhole monitoring and early warning: an experimental and successful GB-InSAR application," *Geomorphology*, vol. 241, no. 241, pp. 304–314, 2015.
- [5] J. Chen, L. Lu, J. Lu, and Y. Luo, "An early-warning system for shipping market crisis using climate index," *Journal of Coastal Research*, vol. 73, pp. 620–627, 2015.
- [6] F. Bode, W. Nowak, and M. Loschko, "Optimization for early-warning monitoring networks in well catchments should be multi-objective, risk-prioritized and robust against uncertainty," *Transport in Porous Media*, vol. 114, no. 2, pp. 261–281, 2016.
- [7] P. Liu, "Development and application of fire safety monitoring and early warning system for small and medium sized hospital enterprises," *Basic and Clinical Pharmacology and Toxicology*, vol. 119, no. 4, Article ID 57, 2016.
- [8] F. Rovero and J. Ahumada, "The tropical ecology, assessment and monitoring (team) network: an early warning system for tropical rain forests," *The Science of the Total Environment*, vol. 574, no. 1, pp. 914–923, 2017.
- [9] Y.-Z. Liu, Y.-S. Zou, Y.-L. Jiang, H. Yu, and G.-F. Ding, "A novel method for diagnosis of bearing fault using hierarchical multitasks convolutional neural networks," *Shock and Vibration*, vol. 2020, no. 13, pp. 1–14, 2020.
- [10] L. Liu, L. Chen, T. Wu, X. Xu, Y. Peng, and W. Chen, "Distribution network operational risk assessment and early warning considering multi-risk factors. IET Generation, Transmission and Distribution," vol. 14, no. 16, pp. 136–154, 2020.
- [11] T. T. de Almeida, J. A. M. Nacif, F. P. Bhering, and J. G. R. Junior, "Doctrams: a decentralized and offline community-based traffic monitoring system," *IEEE Transactions on Intelligent Transportation Systems*, vol. 20, no. 3, pp. 1160–1169, 2019.
- [12] Y. Tang, Z. Qing, L. Zhu, and R. Zhang, "Study on the structural monitoring and early warning conditions of aging jacket platforms," *Ocean Engineering*, vol. 101, no. 1, pp. 152–160, 2015.
- [13] Z. Yang and J. Wang, "A new air quality monitoring and early warning system: air quality assessment and air pollutant concentration prediction," *Environmental Research*, vol. 158, pp. 105–117, 2017.
- [14] T. Carlà, P. Farina, E. Intrieri, K. Botsialas, and N. Casagli, "On the monitoring and early-warning of brittle slope failures in hard rock masses: examples from an open-pit mine," *Engineering Geology*, vol. 228, pp. 71–81, 2017.